

Green's Function Retrieval from the CCF of Random Waves and Energy Conservation for an Obstacle of Arbitrary Shape

Haruo Sato^{1*}

¹Tohoku university, Science, Geophysics

For imaging the earth structure, the cross-correlation function (CCF) of random waves as ambient noise or coda waves has been widely used for the estimation of the Green's function. Here we study the mathematics of the Green's function retrieval in relation to the energy conservation for a single obstacle of arbitrary shape. When an obstacle is placed in a 2-D homogeneous medium, the Green's function is written by a double series expansion using Hankel functions of the first kind which represent outgoing waves. When two receivers and the scattering obstacle are illuminated by uncorrelated noise sources randomly and uniformly distributed on a closed circle of a large radius surrounding them, the lag-time derivative of the CCF of random waves at the two receivers can be written by a convolution of the anti-symmetrized Green's function and the auto-correlation function of the noise source time function. We explicitly derive the constraint for the Hankel function expansion coefficients as the sufficient condition for the Green's function retrieval. We show that the constraint is equivalent to the generalized optical theorem derived from the energy conservation principle. Physical meaning of the generalized optical theorem becomes clear when the Hankel function expansion coefficients are transformed into scattering amplitudes in the framework of the conventional scattering theory.

Sato, H. 2013. Green's Function Retrieval from the CCF of Random Waves and Energy Conservation for an Obstacle of Arbitrary Shape: Noise Source Distribution on a Large Surrounding Shell, *Geophys. J. Int.* in press.

Keywords: Seismic waves, Scattering, structure study, Green function, wave theory

Characteristics of the CCF of coda waves: dependence on the angle between the station pair and the source

Kentaro Emoto^{1*}, CAMPILLO, Michel¹, BRENGUIER, Florent¹, BRIAND, Xavier¹, Tetsuya Takeda²

¹ISTerre, University of Grenoble, France, ²NIED

Coda of earthquakes consists of scattered waves and the late coda can be regarded as a diffuse field. The diffuse wave field is necessary for the seismic interferometry. Campillo & Paul (2003) showed that we can extract the Green's function from field-to-field correlation of coda waves. Different from the noise field, scattered waves around the source region are included in the coda. We analyze the cross-correlation functions (CCF) of coda of earthquakes occurred around the source region of the 2011 Tohoku-oki earthquake and examine the fluctuation of them.

We use the earthquakes with magnitude larger than 5 occurred from 2008 to 2011 and about 74 Hi-net stations located in the east coast of northeastern Japan. We apply the band-pass filter (0.1 - 0.2Hz) and divide the coda window into 300s-long segments from 200s after the origin time until 700s with an interval of overlap of 100s. By stacking the CCFs, we detect the Rayleigh wave with the propagation velocity of 3.2km/s. We examine the dependence on the source location by using the angle between the source and the station pair. The CCFs with angles less than 45 degrees are asymmetry. On the other hand, the CCFs with the angles larger than 45 degrees are more symmetric. This feature was also reported in Paul et al. (2005). This observation indicates that the energy coming from the source is still dominant in the late coda.

We calculate the fractional travel-time change, dt/t , by applying the stretching method to the coda of the CCF and analyze the fluctuation of it. The dt/t shows the strong fluctuation and the RMS of it is about a few percent. This fluctuation is not systematic. The fluctuation of the dt/t measurement based on the stretching method due to the random fluctuation of the waveform is theoretically estimated by Weaver et al (2011). When we apply their theory to our measurement, the predicted fluctuation and the observed fluctuation are the same order of magnitude. This result indicates that the observed fluctuation of dt/t is not reflected the uniform change of the medium. Because the diffuse field of coda is not isotropic, we can't obtain the stable CCF from the coda. We also calculate the CCF of noise field in the same region and calculate the dt/t due to the 2011 Tohoku-oki earthquake by applying the stretching method. We observe the co-seismic change of dt/t . The dt/t increases by about 0.2 % after the earthquake. This is one order of magnitude smaller than the fluctuation of dt/t derived from the CCF of coda. Therefore we can't detect the change due to the earthquake from the CCF of coda. In order to improve the stability of the CCF of coda, we apply the curvelet denoising filter (Stehly et al 2011). By the denoising, the correlation coefficient between each CCF and the stretched reference CCF increases and the fluctuation of the dt/t decreases. However, the fluctuation is still too large to detect the co-seismic change.

Finally, we mention about the signal to noise ratio (SNR) of the CCF. The SNR of the CCF of noise is about 3 times larger than that of the CCF of coda. The ratio of the square root of the length of the time window of the noise used to calculate the one-day CCF to that of the coda is about 14. Therefore, in terms of the length of the time window, the CCF of the coda is efficient to extract the Green's function compared with the noise.

Keywords: Coda wave, Seismic interferometry

Theoretical background for estimating attenuation structures with seismic interferometry

Hisashi Nakahara^{1*}

¹Hisashi Nakahara

Seismic interferometry or the noise correlation method has provided passive methods for travel time tomography. However, it is not clear yet whether amplitudes of Green's functions retrieved from cross correlations can be reliably used to estimate attenuation. Recently, an equation was conjectured by Prieto et al. (2009), which is thought to be an extension of the SPAC method (e.g. Aki, 1957) to lossy media, and it was used to estimate attenuation structures from amplitudes of the retrieved Green's functions. However, the conjecture is not clearly proved yet though numerical and analytical studies are being made. In this study, I prove a theoretical relation between the SPAC method and seismic interferometry for heterogeneous lossy media, and then develop a theory to support the conjecture by the help of the relation. The conjecture turns out to be derived for homogeneous lossy media under two assumptions of (1) weak attenuation and (2) larger station separations than a considered wavelength. Based on the results, applications of seismic interferometry to the estimation of attenuation should be conducted in relatively homogeneous regions with weak attenuation. Applications to attenuation tomography in heterogeneous regions still need to be investigated theoretically.

Acknowledgments

This study was partially supported by JST J-RAPID program.

Keywords: seismic interferometry, SPAC method, attenuation

Seismic interferometric reverse time migration to passive seismic data for subsurface structural survey

Kazuya Shiraishi^{1*}

¹JGI, Inc.

In this study, I propose an imaging method, SI-RTM, for a direct subsurface imaging from passive seismic data by implementing the reverse time migration (RTM) with a concept of the seismic interferometry (SI). The RTM based on a two-way wave equation is a powerful imaging technique in reflection seismic survey for complex subsurface structures, while it takes higher computational cost than conventional migration methods. The RTM principle is represented an imaging condition that the reflected or scattered waves are focused on the imaging points by time integrating the product of two extrapolated wavefields at same recording time; the forward extrapolated wavefield of source wavelet from a source point and the backward extrapolated wavefield of the recorded seismic data from receiver points. The SI is generally used for a redatuming or a signal extraction by crosscorrelating the different seismic traces in a data domain, then the synthesized waveforms are analyzed for wavefield characterization or processed for the subsurface imaging.

The SI-RTM could be recognized as a wavefield interference in an image domain. Instead of the wavefield extrapolation in the conventional RTM, arbitrary time-windowed seismic record is propagated forwards from a receiver point which become a virtual source and is propagated backwards from other receiver points. If any multiple reflecting waves between the surface and the reflection boundaries satisfy the imaging condition, the reflected energy will be focused on subsurface reflection points. The imaging process corresponds to the wavefield extrapolation with a velocity model and interference in the image domain simultaneously. In this study, I evaluated the SI-RTM algorithm by a two-dimensional numerical simulation. Two kinds of synthetic passive seismic data were generated by a finite difference elastic wave modeling; (a) local earthquakes data, and (b) ambient seismic noise data which contain body waves randomly generated. The SI-RTM was implemented under acoustic wavefield condition. Both the test results show validity of the imaging algorithm of SI-RTM.

The SI-RTM needs a velocity model for wavefield extrapolation and takes high computational cost which is dependent on the data volume and the size of a target area. However, it enables us to achieve the direct seismic imaging without source information, and it improves analysis method of the passive seismic data by not only the SI record synthesized in the data domain but also the SI profiles in the image domain when it is difficult to recognize the significant phase on the SI virtual source record. In the engineering aspect, this method will contribute to beneficial use of the passive seismic data in any monitoring projects. In the future work, realistic problems will be overcome by continuing field data study, including further applications such as the imaging of multi-component passive seismic data.

Keywords: reverse time migration, seismic interferometry, passive seismic, reflection seismic survey, numerical simulation

Time-lapse changes in velocity and anisotropy after the 2011 Tohoku earthquake estimated by seismic interferometry

Nori Nakata^{1*}, Roel Snieder¹

¹Colorado School of Mines

Seismologists have estimated time-lapse changes in subsurface velocities and anisotropy caused by the 2011 Tohoku earthquake for two years. Seismic interferometry is recognized as a powerful tool to monitor the velocities and anisotropy, and applied to earthquake records and ambient-noise data recorded by KiK-net, Hi-net, and other seismometers. We apply seismic interferometry to KiK-net data and estimate mean values of near-surface shear-wave velocities in the periods of January 1–March 10 and March 12–May 26 in 2011. We detect about a 5% reduction in the velocity after the Tohoku earthquake. The area of the velocity reduction is about 1,200 km wide, which is much wider than earlier studies reporting velocity reductions after larger earthquakes. The reduction partly recovers with time. We can also estimate the azimuthal anisotropy by detecting shear-wave splitting after applying seismic interferometry. Estimating mean values over the same periods as the velocity, we find the strength of anisotropy increased in most parts of northeastern Japan, but fast shear-wave polarization directions in the near surface did not significantly change. The changes in anisotropy and velocity are generally correlated, especially in the northeastern Honshu (the main island in Japan).

Keywords: seismic interferometry, Tohoku earthquake, time lapse, shear-wave velocity, shear-wave splitting, KiK-net

Computer simulation of high-frequency Po/So propagation in the oceanic lithosphere

Takashi Furumura^{1*}, BLN Kennett²

¹CIDIR/ERI Univ. Tokyo, ²RSES ANU

The phases Po/So are very distinctive high-frequency signals travelling often more than 1000-3000 km through the oceanic lithosphere and recorded at the ocean bottom seismographs with a long coda. We demonstrate that such Po/So signals are developed by multiple forward scattering of high-frequency body P and S wave in heterogeneous oceanic lithosphere based on the analysis of observed set of waveforms and finite-difference simulation of high-frequency seismic wave propagation in heterogeneous structures.

An important component of the propagation is provided by reverberation in the water column and sediments linked to P and S propagation in the oceanic lithosphere. The nature of the observed Po and So phases with high frequencies and long coda is well represented by multiple forward scattering in a lithospheric structure with and quasi-laminate heterogeneity with horizontal scales much larger than vertical.

Despite the generally good propagation of Po/So to stations in the western Pacific such as from the Japan subduction zone to the Wake island ocean bottom stations near Tonga, the propagation in eastern Pacific, e.g., to the H2O station on an old telephone cable between Hawaii and the mainland USA is rather poor for So (Kennett, Zhao and Furumura, 2009). Such poor transmission of the high-frequency Po/So signals along the young (< 25 Ma) oceanic plate can be explained by the ineffective propagation of high-frequency signals in a thinner lithosphere with influence also from oblique propagation across major transform fault systems in the eastern Pacific with changes in lithospheric thickness.

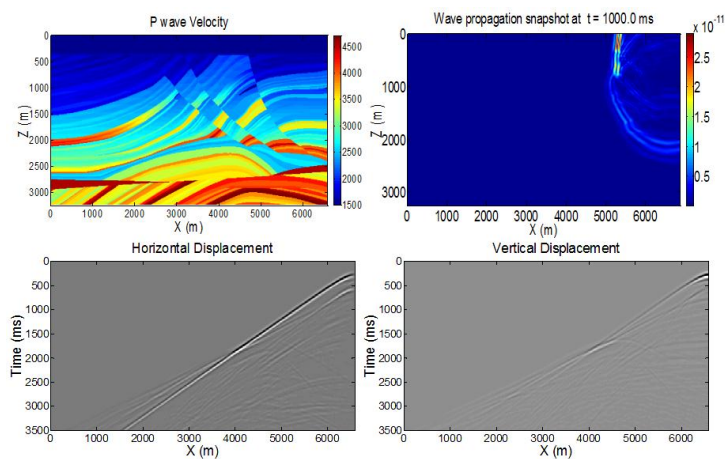
Elastic waveform modeling in frequency domain with an efficient MATLAB code

Ehsan Jamali Hondori^{1*}, Hitoshi Mikada¹, Tada-nori Goto¹, Junichi Takekawa¹

¹Graduate School of Engineering, Kyoto University

Seismic waveform modeling is a key tool to estimate subsurface characteristics, not only for hydrocarbon explorations but also for proper managements of seismic hazards and civil engineering infrastructures. Modeling in frequency domain found to be effective for its numerous advantages compared to that in time domain. Once triangular factors of impedance matrix have been calculated, multiple sources can be processed with the minimum computational costs. Monochromatic and band limited modeling at desired frequencies are implemented in a straightforward manner and the attenuation behavior of elastic media can directly be dealt with considering complex valued elastic parameters. However, discretizing the computational domain requires more grid points to achieve acceptable accuracy and a program with robust algorithm is needed to minimize the modeling time and cost. We used 25-point finite difference stencils to discretize the elastic wave equation in frequency domain to develop an effective MATLAB package for elastic waveform modeling. By using array-processing abilities of MATLAB, we efficiently computed the large impedance matrix for realistic model sizes. In order to solve the system of equations impedance matrix is factorized to lower and upper triangular matrixes, then forward and backward substitution results in horizontal and vertical displacements. Since the impedance matrix has a band structure and very sparse pattern, using efficient ordering schemes to reduce fill-in during factorization is necessary. We used METIS library together with SuiteSparse library for sparse LU factorization. METIS uses a multilevel nested dissection algorithm to calculate a fill reducing ordering which brings a superior performance to the program. SuiteSparse includes several factorization and solution modules, such as UMFPACK, SparseQR, and CHOLMOD, for sparse matrixes and linear system of equations. We used UMFPACK and SparseQR modules in our modeling code for problems with different sizes. Once the factors have been calculated, several seismic sources could be modeled by solving for multiple right hand sides. Reflections from truncated boundaries appear in the solution of the wave equation which must be suppressed by boundary conditions. In order to truncate the computational area we applied Perfectly Matched Layers (PML) on the boundaries. Complex valued velocities based on Kolsky-Futterman model were used to consider attenuation effects in the seismic waveforms. Marmousi2 example (Figure 1) confirmed the efficiency and accuracy of the MATLAB code. We have cropped the original model to focus on the more complex area in the center of the geological model; the final model in the example is 6600 m long and 3200 m deep. A snapshot of wave propagation and shot gathers of horizontal and vertical components of the displacement recorded at the surface are shown in the Figure 1. As is obvious in the horizontal displacement component, strong Rayleigh waves appear in the seismograms and travel near surface with low velocity. Based on the results of Marmousi2 example and several other models which have already tested the program, the developed MATLAB package can be used for fast and accurate elastic waveform modeling.

Keywords: seismic, waveform modeling, frequency domain, finite difference, perfectly matched layers



Amplitude distribution of sP reflected phase from offshore earthquakes in the Pacific side of Tohoku district

Masahiro Kosuga^{1*}

¹Graduate School of Sci. and Tech., Hirosaki Univ.

We observed a prominent phase on vertical seismograms of interplate and intraplate earthquakes offshore Miyagi prefecture with depth ranges from 30 to 60 km. The phase that appears between P- and S-waves is observed widely at stations in the Japan Sea side. Here we examine the waveform and travel times of this phase using Hi-net data and estimate its origin, and discuss potential usage of the phase.

A polarization analysis indicates that the phase has a strike toward the epicenter, nearly vertical dip angle, and large rectilinearity. This indicates that the phase is P-wave coming from the direction of the source. The travel time of the X-phase is proportional to epicentral distance with an apparent velocity of about 7 km/s. This suggests that the reflection/conversion occurs at relatively shallow part. There is no significant azimuthal variation in arrival times of the X-phase, which implies that the plane of reflection/conversion is nearly horizontal. We estimate the position of conversion/reflection by using ordinary hypocenter location method assuming that the phase is P-wave from the conversion/reflection point. The location is near the surface of the coastal area of Miyagi prefecture. The above observational facts of large amplitude, polarization characteristics, apparent velocity, azimuthal variation of arrival times, and the location of conversion/reflection point, are all consistent with an interpretation that the phase is sP reflected phase from the surface. This phase has already found by previous studies and has been used as a depth phase to improve the depth accuracy in hypocenter location and delineate a seismicity pattern along the plate boundary.

Next we investigated amplitude distribution of sP phase. We measured amplitude on RMS envelope as the deviation of smoothly varying envelope. In many cases the amplitude is largest at stations in Akita and Yamagata prefectures, while the amplitude is smaller at stations in the northern and southern part of Tohoku district, and at stations in the Pacific side. The focal mechanisms of these events are reverse faulting with N-S strike. In the case of reverse faulting earthquake with E-W strike, the area of large amplitude shifts to the northern part of Tohoku district. This indicates that the amplitude distribution of sP phase depends on focal mechanisms. Thus the amplitude of sP phase has a potential usage to determine focal mechanisms of offshore earthquakes, which is difficult from the P-wave polarization only.

Acknowledgement: We thank the National Research Institute for Earth Science and Disaster Prevention (NIED) for providing waveform data from Hi-net.

Keywords: sP wave, reflection, amplitude, focal mechanisms

Effect of brine viscosity on ultrasonic wave attenuation

Jun Matsushima^{1*}

¹The University of Tokyo

Seismic attenuation is a highly variable physical parameter that depends on confining pressure, porosity, degree of fluid saturation, and variations in fluid properties such as elastic modulus, viscosity, and polarity. In our previous paper, we used partially frozen brine as a solid-liquid coexistence system to investigate seismic attenuation phenomena. Ultrasonic wave transmission measurements on this ice-brine coexisting system were conducted to examine the influence of unfrozen brine in the pore microstructure of ice on ultrasonic waves. From liquid phase to around the freezing point, the presence of a partially frozen brine increases both velocity and attenuation. During the growth of ice from brine, salt cannot incorporate into the ice crystals. As the ice freezes, the salt is rejected and concentrates in the brine; thus, as the salinity increases in the brine filled pores, the freezing point of the remaining fluid is successively lowered and furthermore the viscosity of remaining high salinity unfrozen brines becomes larger and larger. Seismic attenuation related to viscous effect is caused by relative fluid-solid motion is one of the most important attenuation mechanisms. This paper is concerned with the effect of such viscosity on attenuation at ultrasonic frequencies. We observed the variations of a transmitted wave, changing its salinity and quantitatively estimated attenuation for unconsolidated porous material saturated with brine by considering different distances between the source and receiver transducers. The waveform analyses for P-waves indicate that the attenuation increases with increasing salinity (i.e. increasing viscosity). In order to elucidate the physical mechanism responsible for ultrasonic wave attenuation measured at different salinity (i.e. different viscosity), we employ a poroelastic model based on the Biot theory to describe the propagation of ultrasonic waves through partially frozen brines.

Keywords: Seismic attenuation, viscosity, poroelastic

Characteristics of high-frequency seismic waves during relatively deep event at Kanto region

Shunsuke Takemura^{1*}, Kazuo Yoshimoto¹

¹Yokohama City University

Observed Characteristics of high-frequency seismic waves

Observed records during Mw 5.0 earthquake occurring at depth of 53 km at southwestern Ibaraki, central part of Japan, demonstrated various features depending on the station location. Especially, the waveforms with 2-4 Hz at central and southern part of Chiba are showing strong peak delay and spindle shape of S wave, while weak peak delay appears at other area in Kanto region. In the high frequency ($f > 1$ Hz), seismic waves are strongly affected by the effect of seismic wave scattering due to small-scale velocity fluctuation along propagation path (e.g. Sato, 1989). The spatial distribution of small-scale velocity fluctuation in the subsurface structure of Kanto area may be cause of strong peak delay (e.g., Takahashi et al., 2007).

2-D FDM simulation

We conduct FDM simulation of seismic wave propagation in the 2-D heterogeneous structure to clarify the cause of strong peak delay. Our 2-D simulation model is covering the zone 245 by 123 km, which has been discretized with grid size 0.015 km. We assume the layered background velocity structure base on the model proposed by Koketsu et al. (2008). The model is including basin structure, crust, mantle and subducting oceanic plate.

In order to introduce the effect of seismic wave scattering, we assume stochastic random velocity fluctuation in each layer. Random velocity fluctuations are characterized by exponential-type auto-correlation function (ACF) with correlation distance $a = 3$ km and strength of fluctuation $e = 0.05$ in the upper crust, $a = 3$ km and $e = 0.07$ in the lower crust, $a = 10$ km and $e = 0.02$ in the mantle (e.g., Takemura and Furumura, 2013). In the subducting plate, we assume anisotropic random velocity fluctuation characterized by exponential-type ACF with $a_H = 10$ km in horizontal direction, $a_Z = 0.5$ km in vertical direction and $e = 0.02$ (Furumura and Kennett, 2005). In the low velocity layer, basin structure, we assume random velocity fluctuation model characterized by exponential-type ACF with $a = 1$ km in vertical direction and $e = 0.07$.

In addition, we assume the low-velocity zone at northeastern part of Chiba with depth of 30 km (Matsubara et al., 2004). In the low-velocity zone, random velocity fluctuation characterized by Gaussian-type ACF with $a = 0.5$ km and $e = 0.10$ is superposed on exponential-type ACF with $a = 3$ km and $e = 0.07$. Strong seismic scattering would occur in the low-velocity zone of simulation model and affect peak delay time at Chiba.

Simulation results

Simulated waveforms with 2-4 Hz are showing spindle shape due to scattering and energy trap in the basin structure. Strong peak delay also appears at central and southern part of Chiba. Simulation result demonstrated that strong scatters in the low velocity zone play important role in peak delay time and waveform shape.

Low-velocity zone at northeastern Chiba is considered as a result of dehydrated water from oceanic crust of subducted Philippine Sea plate. Therefore strong small-scale velocity fluctuation in the low-velocity zone may be related with dehydrated water.

Acknowledgement

We acknowledge the National Research Institute for Earth Science and Disaster Prevention, Japan (NIED) for providing the K-NET/KiK-net waveform data. The computations were conducted on the Earth Simulator at the Japan Marine Science and Technology Center (JAMSTEC).

Keywords: seismic wave, numerical simulation, seismic wave scattering, heterogeneous subsurface structure

Tsunami-induced ground tilt changes observed by Hi-net and F-net in Japan

Takeshi Kimura^{1*}, Sachiko Tanaka¹, Tatsuhiko Saito¹

¹National Research Institute for Earth Science and Disaster Prevention

Oscillating ground tilt perturbations accompanied by the 2010 Maule, Chile, earthquake tsunami were observed over a broad inland area facing the Pacific Ocean coast in Japan by high-sensitivity accelerometers of Hi-net (Kimura et al., 2013, JGR) and broadband seismometers of F-net. In the present study, we investigated the characteristics of the ground tilt changes induced by the Maule earthquake tsunami using the Hi-net tiltmeter records. The very dense network throughout Japan revealed the precise distribution of the tsunami-induced perturbations. To demonstrate the link between the tsunami and the observed inland tilt changes, we also simulated the deformation of the solid Earth due to the ocean loading disturbances caused by the tsunami. Furthermore, based on our observations and a simple tsunami model, we discussed possible uses of land data in characterizing tsunami behavior, particularly in nearshore environments.

Through an analysis of ground tilt data observed at more than 500 Hi-net stations, we were able to obtain a detailed spatiotemporal distribution of the tsunami-induced tilt changes and reveal a relationship between the tilt amplitude and the distance from the coast. At distances of 1 km or less, the peak tilt amplitudes were $\sim 5 \times 10^{-8}$ rad and were almost constant with respect to the distance. At distances greater than 3 km, amplitudes were inversely proportional to the distance and reached $\sim 5 \times 10^{-9}$ rad approximately 50 km away from the coast. The dominant ground tilting directions were almost the same as the direction orthogonal to the coastline. The tsunami-induced signals were also observed at F-net stations in coastal area and small islands.

These observed ground tilt changes and their characteristics were successfully modeled with a loading deformation caused by sea level variations accompanied by the tsunami. Applying a two-dimensional boxcar tsunami model to the observed data, we estimated the water volume per unit length of coast for the Maule earthquake tsunami to be $2-7 \times 10^3 \text{ m}^3/\text{m}$ within the distance of 14-20 km seaward of the coastline.

Tsunami generation and propagation due to sea-bottom deformation: A linear potential theory

Tatsuhiko Saito^{1*}

¹NIED

The present study obtained a solution of the velocity potential for sea-bottom deformation with an arbitrary source time function for constant water depth. By using this velocity potential, we theoretically derived semi-analytical solutions of the velocity distributions in the sea, the water height at the surface, and the pressure at the bottom. The velocity distribution is represented by the sum of the direct and indirect components excited from the sea-bottom deformation: the direct component is the velocity distribution excited directly from the sea-bottom deformation and the indirect component the velocity distribution excited from the water height distribution at the surface. The semi-analytical solution indicates that the direct component should be zero or the initial velocity distribution be zero as the initial condition for 2-D tsunami propagation simulations. The pressure at the bottom is represented by the sum of hydrostatic and dynamic components. When the sea-bottom uplifts with an increasing rate, the sea-bottom pressure becomes larger than the hydrostatic pressure. This is noteworthy when we rapidly estimate a magnitude of tsunami by analyzing ocean-bottom pressure gauges deployed inside a focal region.

Keywords: tsunami, linear theory